Magnetic and transport properties of degenerate ferromagnetic semiconductor EuO

Masao Takahashi*

Kanagawa Institute of Technology, 1030 Shimo-Ogino, Atsugi-shi, 243-0292, Japan

(Received 26 December 2015; revised manuscript received 11 May 2016; published 13 June 2016)

By applying the coherent potential approximation (CPA) to simple models, we have studied the temperature (T) dependence of the normalized magnetization $M(T)$, and electrical resistivity $\rho(T)$ of highly rare-earth-doped EuO. The present result reveals that in degenerate EuO, the magnetization is described by an electron-doped EuO model; the strong double-dome feature of $M(T)$ of Gd-doped EuO is a consequence of the half-metallicity and low dopant activation. In degenerate EuO, the temperature dependence of the resistivity is well described by Matthiessen's rule as $\rho(T) = \rho_C + \rho_m(M)$, where ρ_C is the nonmagnetic scattering contribution (independent of T) and $\rho_m(M)$ is the magnetic scattering contribution due to the exchange interaction with localized f spins. ρ_C is proportional to $x(1-x)/n^{\frac{2}{3}}$, while the amplitude of the change in $\rho_m(M)$ is proportional to $n^{-\frac{2}{3}}$, where x is the doped rare-earth density and n is the electron density. The difference in $M(T)$ and $\rho(T)$ between Gd- and La-doped EuO is also discussed.

DOI: 10.1103/PhysRevB.93.235201

I. INTRODUCTION

Research interest in the ferromagnetic semiconductor EuO has been renewed in recent years as a result of modern techniques and improved sample quality. Since the Curie temperature (T_C) of stoichiometric EuO is about 70 K, for spintronic applications, increasing T_C is the key issue to be addressed. To increase T_C, rare-earth doping with trivalent ions such as La and Gd has been extensively studied [1–5].

In our previous study [6], we theoretically studied the electronic and magnetic properties of Gd-doped EuO by applying the dynamical coherent potential approximation (dynamical CPA) to electron-doped EuO and $Eu_{1-x}Gd_xO$ models. We calculated the density of states (DOS), the normalized magnetization $M(T)$ as a function of the temperature T, and the enhanced T_C as a function of the electron density n (assuming $n = x$). The previous result clarified the nature and properties of the magnetic impurity states and/or impurity band tail of $Eu_{1-x}Gd_xO$ in the dilute region of $x \lesssim 0.50\%$, suggesting a threshold Gd concentration x_C for increasing T_C. The results also clarified that an attractive on-site potential E_C makes the anomalous shape of $M(T)$ less clear and suppresses the increase in T_C. The previous result with the value of E_C that reproduces a shallow donor is, however, somewhat inconsistent with the experimental observation for $M(T)$ in degenerate samples [1]. The consistency may be improved by taking account of the reduction in E_C owing to the screening effect in degenerate EuO. Furthermore, we need to investigate the effect of low dopant activation (or $n < x$) that was experimentally observed [2]. In addition, we calculate the electrical resistivity ρ for comparison with the experimental observations [3]. On the basis of a modified model, in this study, we also discuss the similarities and differences between Gd-doped EuO and La-doped EuO.

II. BASIC CONSIDERATION

In the previous study, we investigated the electron states in $Eu_{1-x}Gd_xO$ using the following Hamiltonian:

$$H_t = \sum_{m,n,\mu} \varepsilon_{mn} a^\dagger_{m\mu} a_{n\mu} + \sum_n u_n + H_f \ , \tag{2.1}$$

where H_f is a Heisenberg-type Hamiltonian for the ferromagnetism of pure EuO with Curie temperature $T_C = 70$ K. The notation here is conventional and the same as that in our previous paper [6]. The first term in Eq. (2.1) represents the kinetic energy of an electron; in our CPA calculation, ε_{mn} appears only through the unperturbed DOS. Thus we employ a simple model DOS given by

$$D_0(\varepsilon) = \frac{2}{\pi\Delta}\sqrt{1-\left(\frac{\varepsilon}{\Delta}\right)^2} \tag{2.2}$$

instead of the true DOS related to the Bloch band structure with ε_{mn}. The second term represents the local potential at the nth site; u_n is either u_n^{Eu} (at the Eu site) or u_n^{Gd} (at the Gd site) depending on the ion species occupying the nth site:

$$u_n^{\mathrm{Eu}} = -I \sum_{\mu,\nu} a^\dagger_{n\mu} \boldsymbol{\sigma}_{\mu\nu} \cdot \mathbf{S}_n a_{n\nu} \ , \tag{2.3}$$

$$u_n^{\mathrm{Gd}} = -E_C \sum_{\mu} a^\dagger_{n\mu} a_{n\mu} - I \sum_{\mu,\nu} a^\dagger_{n\mu} \boldsymbol{\sigma}_{\mu\nu} \cdot \mathbf{S}_n a_{n\nu} \ . \tag{2.4}$$

In the present work, we study the electron states in $Eu_{1-x}La_xO$ by replacing u_n^{Gd} in the above model Hamiltonian by u_n^{La}:

$$u_n^{\mathrm{La}} = -E_C \sum_{\mu} a^\dagger_{n\mu} a_{n\mu} \ . \tag{2.5}$$

In brief, the difference between u_n^{La} and u_n^{Gd} is the absence/presence of the exchange interaction at the impurity site.

Similar Hamiltonians have been widely used by many authors. When the impurity density is $x = 0$, the model expressed by Eq. (2.1) is called the s-f model or Kondo lattice model, which is currently accepted as a basis for studying the conduction electron states and ferromagnetism in the magnetic semiconductors EuO and EuS [7–10]. The present model is an

*taka@gen.kanagawa-it.ac.jp

extension of the s-f model and is applicable to EuO doped with magnetic and/or nonmagnetic impurities [6,11,12]. When H_f is absent, the present model with the nonmagnetic impurity corresponds to the model that is employed to study the optical properties of II-VI diluted magnetic semiconductors (DMSs) [13] and the carrier-induced ferromagnetism in III-V DMSs [14–23]. These models have three key features: (i) an exchange interaction between a conduction electron and localized spins, (ii) the random substitution of magnetic and/or nonmagnetic impurities, and (iii) the thermal fluctuation of localized spins. Since the essential physics involves an exchange interaction with intermediate coupling strength and bound-state formation, a perturbative approach is not available. Some methods have been devised that go beyond the perturbative treatment, one of which is the dynamical CPA.

The dynamical CPA can simultaneously treat substitutional disorder and the thermal fluctuation of the localized spin system. In the dynamical CPA [6,24], the thermal average of a physical quantity, such as Green's function, over a fluctuating localized f spin is taken under the effective field that produces $\langle S_z\rangle$, where $\langle S_z\rangle$ is the thermal average of the localized f spin. Thus the electron state is described in terms of $\langle S_z\rangle$; the T dependence is obtained through $\langle S_z\rangle$. The spin-flip/spin-nonflip process of an electron through the exchange interaction with the f spin is appropriately taken into consideration in the single-site approximation. Thus the dynamical CPA is applicable to the case of sufficiently low Gd doping for an impurity band to form. In the classical spin limit, the numerical results obtained by the dynamical CPA are in good agreement with those obtained by dynamical mean-field theory (DMFT) [21,22]. It has also been reported that the result for optical conductivity obtained by the dynamical CPA is in reasonable agreement with that obtained by Monte Carlo (MC) simulation [23].

The procedure to calculate the DOS for a given normalized magnetization $M[\equiv\langle S_z/S\rangle]$ and the normalized magnetization as a function of the temperature $M(T)$ was presented in our previous study [6]. Throughout our studies, we set $S = 7/2$ for localized f spins and the exchange energy $IS \equiv I_{df} \times S = 0.1 \times 7/2 = 0.35$ eV [25]. We also assume a broad bandwidth of $2\Delta = 7.0$ eV (i.e., $IS/\Delta = 0.1$) so as to reproduce a magnetic redshift of 0.27 eV. In the previous study, we set the on-site potential $E_C = 0.5\Delta$ for a Gd ion so as to produce a shallow donor level that corresponds to the activation energy experimentally observed in a nondegenerate sample of Gd-doped EuO [25]. In a degenerate sample, however, the value of E_C may differ from 0.5Δ. The on-site potential E_C originates from the Coulomb attraction between a donor electron and a trapping center. With increasing x and/or n, the Coulomb attraction is screened and becomes less effective. For DMSs, to consider the dependence of E_C on x, Popescu *et al.* assumed a phenomenological x-dependent on-site potential [21]. Instead of an x-dependent E_C, in the present work, we treat E_C as a parameter to investigate the screening effect. Furthermore, by choosing an appropriate value for E_C, we attempt to consistently explain the magnetic and transport properties of rare-earth-doped EuO.

It is very difficult to calculate the electrical resistivity within the framework of the single-site approximation while taking the long-range property of the Coulomb potential into account [26–28]. Therefore, employing an on-site E_C for the attractive potential at the Gd site in the present study, we first study the conditions for which Matthiessen's rule holds, and then investigate the x and/or n dependence of the resistivity. Assuming that electrons are degenerate, we calculate the electrical resistivity $\rho = 1/(\sigma_\uparrow + \sigma_\downarrow)$ using [28–31]

$$\sigma_\mu = \sigma_0 \times \Delta \int_{-\Delta}^{\Delta} d\varepsilon \left(\mathrm{Im}\frac{1}{\varepsilon_\mathrm{F} - \varepsilon - \Sigma_\mu}\right)^2 \left[1 - \left(\frac{\varepsilon}{\Delta}\right)^2\right]^{\frac{3}{2}}, \tag{2.6}$$

where ε_F is the energy of the Fermi level obtained if the electron density n is given and $\Sigma_\mu[\equiv\Sigma_\mu(\varepsilon_\mathrm{F})]$ is the spin-dependent coherent potential ($\mu = \uparrow$ or $\downarrow$); $\sigma_0 = 4e^2/9\pi^2\hbar a = 2.132 \times 10^4 (1/\Omega\cdot\mathrm{m})$ for EuO with a rock-salt crystal structure with $a = 5.141$ Å. The complex medium Σ_μ is calculated by the dynamical CPA for a given value of M. Since M is a function of T, we can describe ρ in terms of T. Since the CPA is a single-site approximation, the effect of the short-range ferromagnetic order is beyond the scope of this study [32,33].

III. RESULTS AND DISCUSSION

To study the effect of E_C, in Fig. 1, we show the resistivity as a function of the temperature $\rho(T)$ calculated for $Eu_{1-x}Gd_xO$ with $x = 5.0\%$ assuming $n = 1.5\%$ for various values of E_C. The result shows that $\rho(T)$ strongly depends on E_C. The difference in $\rho(T)$ between low and high temperatures $|\rho(\infty) - \rho(0)|$ is 2.9×10^{-6} Ω m and almost constant in the range of $E_C \lesssim 0.30\Delta$, but it increases with increasing $E_C(\gtrsim 0.30\Delta)$; it takes values of 5.0×10^{-6} and 7.2×10^{-6} Ω m for $E_C = 0.40\Delta$ and 0.50Δ, respectively. This suggests that when $E_C \lesssim 0.30\Delta$, $\rho(T)$ can be written by Matthiessen's rule as $\rho(T) = \rho_C + \rho_m(M)$, where ρ_C is the nonmagnetic scattering contribution due to the on-site potential at the substitutionally disordered Gd site and $\rho_m(M)$ is the magnetic scattering contribution due to the exchange interaction with localized f spins. $\rho_m(M)$ depends on T through $M(T)$. In degenerate Gd-doped EuO samples, the total resistivity can be written as $\rho_t(T) = \rho_i + \rho_l(T) + \rho_m(M)$, where $\rho_l(T)$ is the lattice-scattering contribution (linear in T) [34]. ρ_i may include not only ρ_C but also the nonmagnetic scattering due to vacancies. Comparison between the ratio of ρ_C to $|\rho(\infty) - \rho(0)|$ shown in Fig. 1 and the experimental observation suggests that $E_C \sim 0.15\Delta$ in degenerate Gd-doped EuO.

In Fig. 2(a), the $M(T)$ curve of $Eu_{1-x}Gd_xO$ for $x = 5.0\%$ with $n = 1.5\%$ is shown for various E_C. The result shows that when $E_C \lesssim 0.20\Delta$ the $M(T)$ curve is substantially determined by n and well described by the electron-doped EuO model (i.e., $E_C = 0$ or $x = 0$), but when E_C increases beyond 0.20Δ, the $M(T)$ curve deviates from that of the electron-doped EuO model to suppress the increase in T_C. The result in Fig. 2(b) shows that the $M(T)$ curve is well described by the electron-doped EuO model for a wide range of n when $E_C \lesssim 0.20\Delta$.

For a long time, it was widely accepted that each Gd^{3+} ion substituted for Eu^{2+} acts as a donor and donates one electron to the conduction band in Gd-doped EuO. However, Mairoser *et al.* experimentally showed that the fraction of active dopants is $p \equiv n/x \approx 0.30$ for $0.014 \leqslant x \leqslant 0.10$, indicating that only

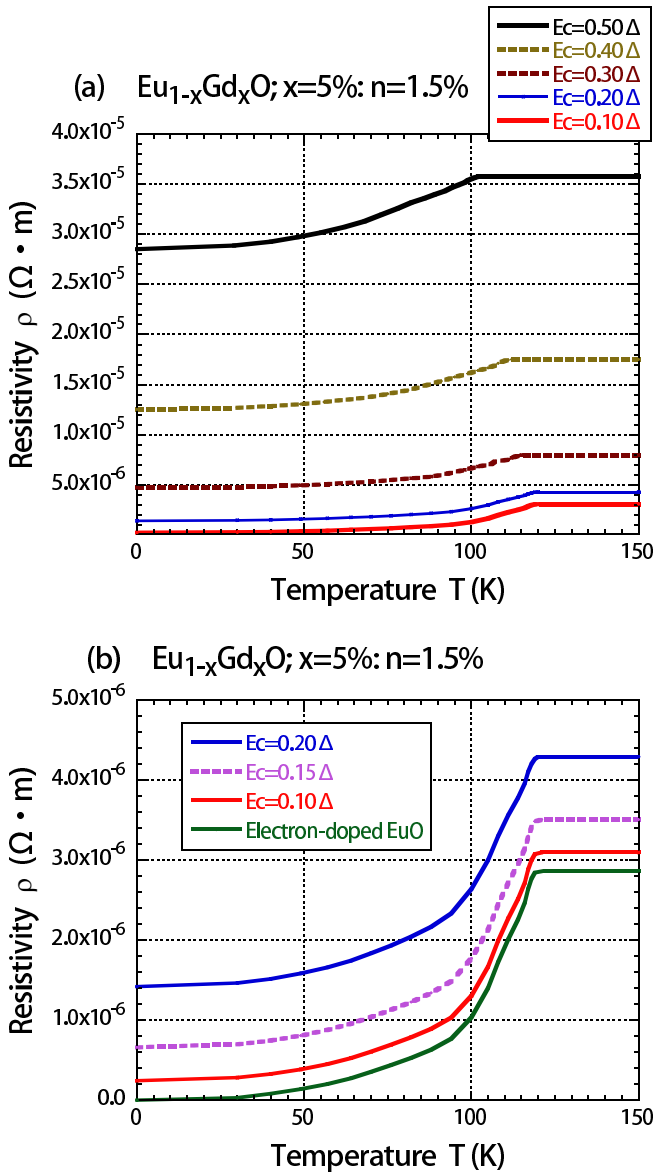

FIG. 1. Temperature dependence of resistivity $\rho(T)$ of $Eu_{1-x}Gd_xO$ with $x = 5.0\%$ and $n = 1.5\%$ for various on-site potentials E_C; (a) $E_C = 0.50\Delta$, 0.40Δ, 0.30Δ, 0.20Δ, and 0.10Δ; (b) $E_C = 0.20\Delta$, 0.15Δ, 0.10Δ, and 0. Note that the scales of the vertical axes in (a) and (b) are different.

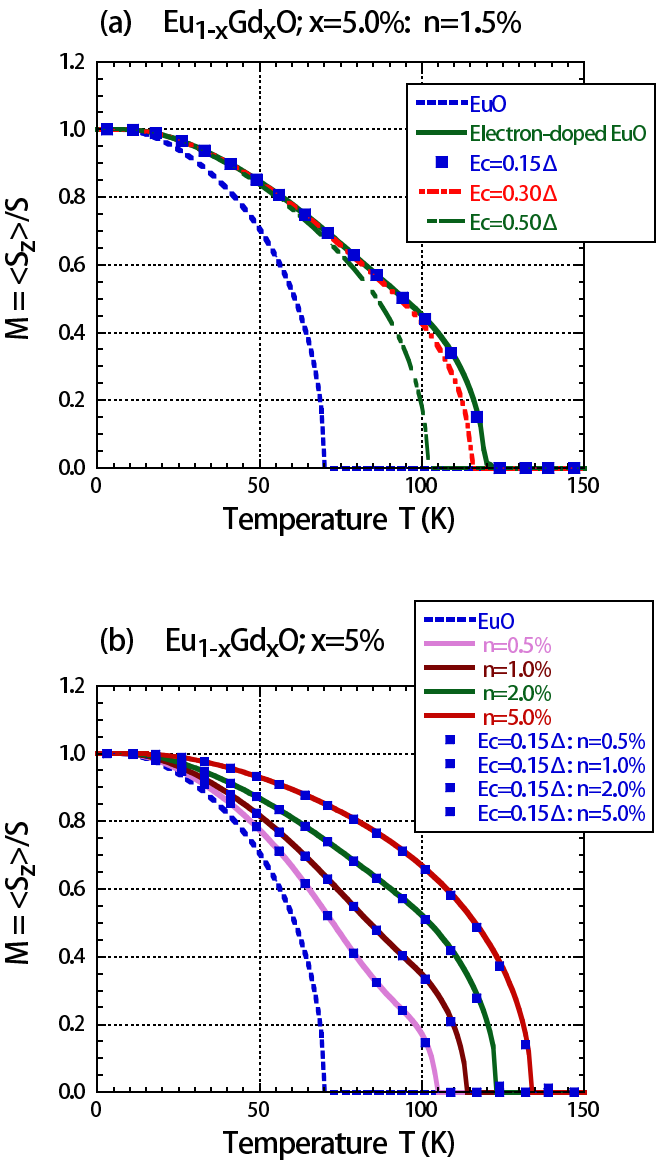

FIG. 2. Temperature dependence of normalized magnetization $M(T)[\equiv \langle S_z\rangle/S]$ of $Eu_{1-x}Gd_xO$ calculated with $x = 5.0\%$: (a) $M(T)$ calculated with $n = 1.5\%$ for $E_C = 0.0$, 0.15Δ, 0.30Δ and 0.50Δ and (b) $M(T)$ calculated with $n = 0.5\%$, 1.0%, 2.0%, and 5.0% for $E_C = 0.0$ and 0.15Δ. $M(T)$ for EuO with $T_C = 70$ K is included for comparison.

a small fraction of introduced Gd may donate electrons to the conduction band [2]. For comparison with the experimental observation, therefore, assuming $n = 0.30x$ for $x < 10\%$, we calculate $M(T)$ and $\rho(T)$ for $Eu_{1-x}Gd_xO$ with $E_C = 0.15\Delta$. As shown in Fig. 3(a), the result for $M(T)$ is in good agreement with that for the electron-doped EuO model for a wide range of x and/or n. This implies that the effect of E_C on $M(T)$ is negligible in degenerate Gd-doped EuO. Note that the double-dome shape of $M(T)$ appears when $x \lesssim 3.0\%$ owing to the assumption of a low election density of $n \lesssim 0.9\%$. The double-dome feature of $M(T)$ is strongly related to the half-metallicity that is caused by the exchange splitting of the band [35,36]. As was shown in the previous study [6], when $n = x$, the double-dome feature of $M(T)$ occurs in a very narrow range of $x \lesssim 1\%$, which is inconsistent with the experimental observation [1]. It is also worth noting that the double-dome shape of $M(T)$ does not occur if we assume $E_C = 0.50\Delta$ (see Fig. 15(a) in Ref. [6]). Therefore the double-dome shape of $M(T)$ is closely related to the low value of n owing to low dopant activation and the inefficiency of the on-site potential in degenerate EuO.

The result for $\rho(T)$ shown in Fig. 3(b) is interpreted assuming $\rho(T) = \rho_C + \rho_m(M)$ as below. $\rho_m(M)$ depends on T through $M(T)$. Note that $\rho_m(1) = 0$; thus, $\rho_m(0)$ is the magnitude of the change in the resistivity due to magnetic scattering. $\rho_m(0)$ decreases with increasing n. Therefore the increase in x accompanying an increase in n results in a decrease in $\rho(0)$. Thus the present result with $n = 0.3x$ for $x \leqslant 7.0\%$ explains the lowering of $\rho(T)$ at high temperatures

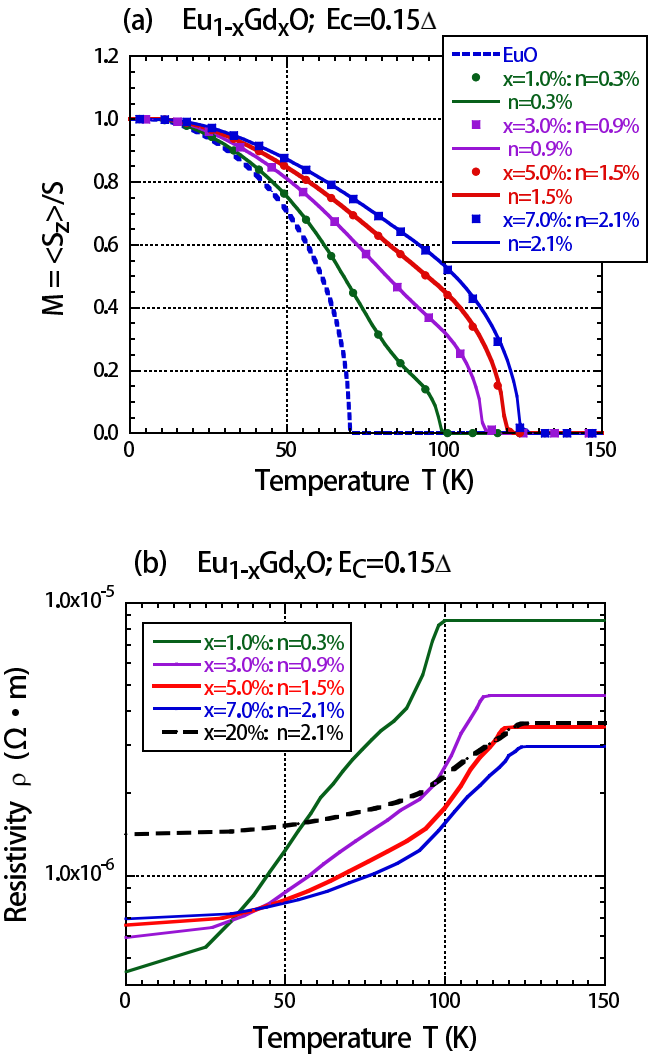

FIG. 3. Results calculated for $Eu_{1-x}Gd_xO$ with $E_C = 0.15\Delta$ for various combinations of values of n and x: (a) $M(T)$ and (b) $\rho(T)$. Note that in (b), $\rho(T)$ is plotted on a logarithmic scale.

as shown in Fig. 3(b). On the other hand, ρ_C is independent of T and proportional to $x(1-x)$. This means that $\rho(T)$ depends not only on n but also on x. It has been experimentally shown that further increasing x to over 10% is not accompanied by an increase in n [2]. To investigate the interplay between n and x, we calculate $\rho(T)$ for $x = 20\%$ and 7.0% while fixing $n = 2.1\%$; the calculated value of $\rho(T)$ for $x = 20\%$ is larger than that for $x = 7.0\%$ owing to the increase in ρ_C. The result shown in Fig. 3(b) well explains the experimental observation that the resistivity strongly depends on x with a minimum at $x \sim 10\%$ [2].

Here, we discuss the behavior of $\rho(T)$ in more detail on the basis of Matthiessen's rule. Assuming $E_C = 0$, we first calculate $\rho_m(0)$ or the resistivity due to the exchange interaction at paramagnetic temperatures in the electron-doped EuO model. In Fig. 4, we show the result for $\rho_m(0)$ as a function of n, together with the result for $|\rho(\infty) - \rho(0)|$ shown in Fig. 3(b). The comparison between the results shows that we can approximately treat $|\rho(\infty) - \rho(0)|$ as $\rho_m(0)$, which means that a finite value of E_C $(= 0.15\Delta)$ does not affect

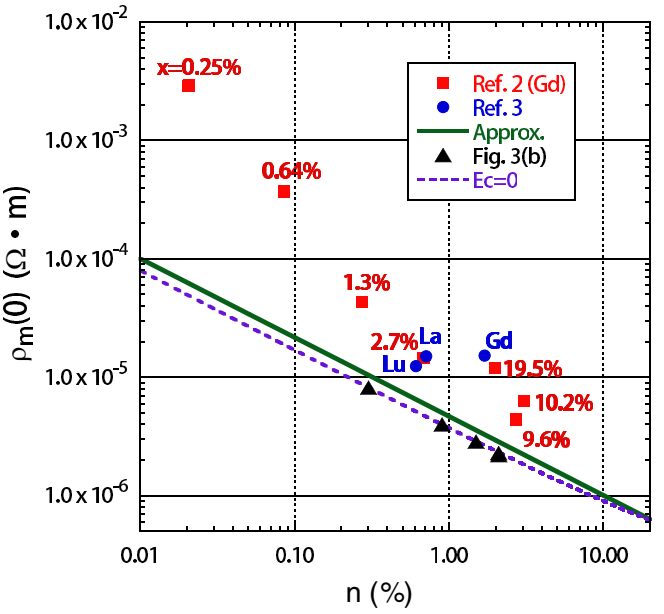

FIG. 4. Amplitude of the change in the resistivity due to magnetic scattering $\rho_m(0)$ as a function of electron density n. The dashed line shows the results assuming $E_C = 0$, while the solid line shows the result calculated using the approximate equation Eq. (3.3). The triangles represent $|\rho(\infty) - \rho(0)|$ shown in Fig. 3(b). The experimental results estimated from the data of $Eu_{1-x}Gd_xO$ with $x = 0.25\%$, 0.64%, 1.3%, 2.7%, 9.6%, 10.2%, and 19.5% in Ref. [2], and the data of 5% Lu-doped, 5% La-doped, and 5% Gd-doped EuO in Ref. [3] are included (see text).

$|\rho(\infty) - \rho(0)|$. When IS/Δ is sufficiently small, $\rho_m(M)$ is given by [37]

$$\rho_m(M) = \rho_m(0) \cdot \frac{(1-M^2)[(1+1/S)^2 - M^2)]}{(1+1/S)(1+1/S-M^2)}. \quad (3.1)$$

$\rho_m(M)/\rho_m(0)$ is a function of M, while its function form does not strongly depend on IS/Δ. When IS/Δ is small, $\rho_m(0)$ is given by

$$\rho_m(0) = \frac{\rho_0}{\pi} \frac{1}{\left[1 - \left(\frac{\varepsilon_F}{\Delta}\right)^2\right]^{\frac{3}{2}}} \left| \frac{\mathrm{Im}\Sigma(\varepsilon_F)}{\Delta} \right| \quad (3.2)$$

with $|\frac{\mathrm{Im}\Sigma(\varepsilon_F)}{\Delta}| = 2(\frac{IS}{\Delta})^2(1+\frac{1}{S})[1-(\frac{\varepsilon_F}{\Delta})^2]^{\frac{1}{2}}$, where $\rho_0 = 1/\sigma_0 = 4.690 \times 10^{-5}\Omega \cdot \mathrm{m}$. When n is sufficiently small, we can set $[1-(\frac{\varepsilon_F}{\Delta})^2] \approx (\frac{3\pi n}{4})^{\frac{2}{3}}$ for the model DOS given by Eq. (2.2). Therefore, when n is sufficiently small, $\rho_m(0)$ is given by

$$\rho_m(0) = \frac{2}{\pi}\left(\frac{4}{3\pi}\right)^{\frac{2}{3}}\left(\frac{IS}{\Delta}\right)^2\left(1+\frac{1}{S}\right)\frac{\rho_0}{n^{\frac{2}{3}}}. \quad (3.3)$$

The result for $\rho_m(0)$ obtained using Eq. (3.3) is shown in Fig. 4, together with the result estimated from the data in Refs. [2] and [3]. Note that in the data in Ref. [3], not only the data for Gd-doped EuO but also the data for La- and Lu-doped EuO are included. Figure 4 suggests that $\rho_m(0)$ estimated from the experimental data for degenerate samples ($n \gtrsim 0.1\%$) is roughly proportional to $n^{-\frac{2}{3}}$.

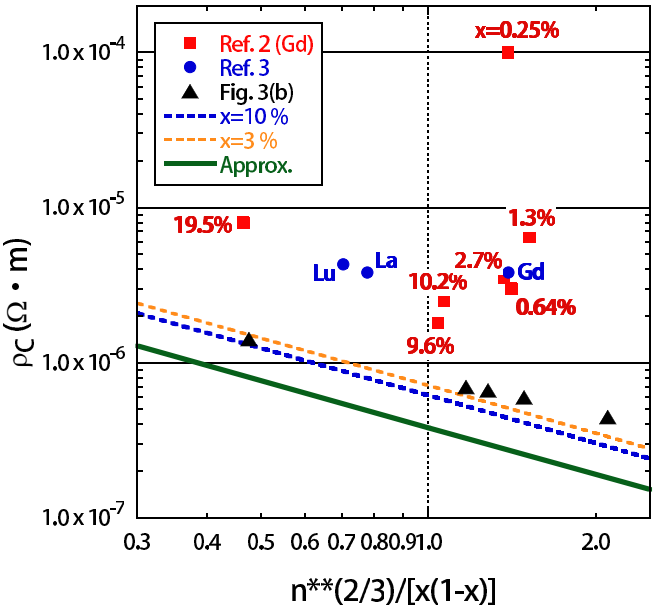

FIG. 5. ρ_C calculated as a function of $n^{\frac{2}{3}}/[x(1-x)]$. The dashed lines show the results obtained assuming $IS = 0$ with $x = 10\%$ and 3%, while the solid line shows the result calculated using the approximate equation Eq. (3.4). The triangles represent ρ_C shown in Fig. 3(b). The experimental results estimated from the data of $Eu_{1-x}Gd_xO$ with $x = 0.25\%$, 0.64%, 1.3%, 2.7%, 9.6%, 10.2%, and 19.5% in Ref. [2], and the data of 5% Lu-doped, 5% La-doped, and 5% Gd-doped EuO in Ref. [3] are included (see text).

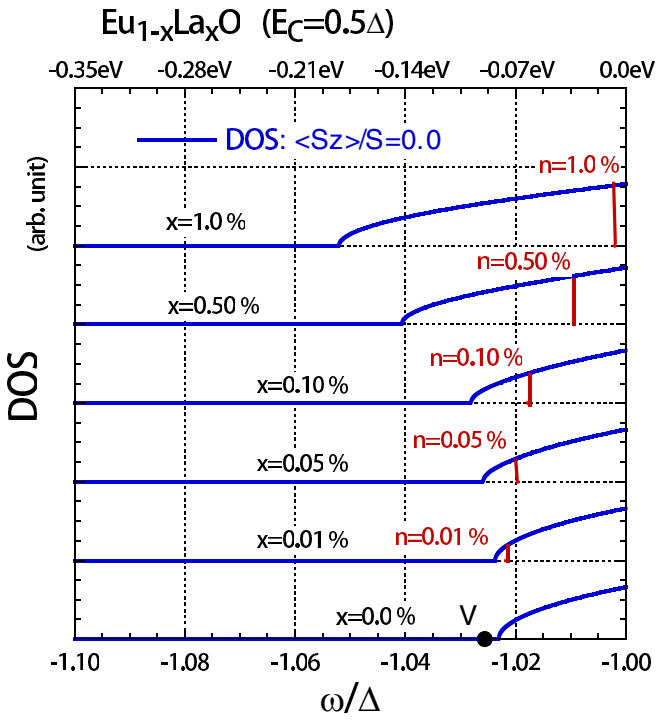

FIG. 6. Lower-energy part of DOS at paramagnetic temperatures for various impurity densities x of $Eu_{1-x}La_xO$ ($E_C = 0.5\Delta$). The vertical lines indicate the Fermi levels for $n = x$. The dot V indicates the impurity level for $x \to 0$.

To investigate the effect of E_C on ρ_C, we next calculate ρ_C assuming $IS/\Delta = 0$. This problem is equivalent of that of a random binary alloy A_xB_{1-x} with offset energy E_C. In Fig. 5, we present the results for ρ_C with $IS/\Delta = 0$ for $x = 10\%$ and 3% as a function of $n^{\frac{2}{3}}/[x(1-x)]$. The comparison between ρ_C with $IS/\Delta = 0$ and that calculated with $IS/\Delta = 0.1$ for various x and n shown in Fig. 3(b) suggests that the spin polarization of the band does not strongly affect ρ_C. When E_C/Δ is small, $|\frac{\mathrm{Im}\Sigma(\varepsilon_F)}{\Delta}| = 2x(1-x)(\frac{E_C}{\Delta})^2[1-(\frac{\varepsilon_F}{\Delta})^2]^{\frac{1}{2}}$. Furthermore, when n is sufficiently small, ρ_C is therefore given by

$$\rho_C = \frac{2}{\pi}\left(\frac{4}{3\pi}\right)^{\frac{2}{3}}\left(\frac{E_C}{\Delta}\right)^2 \frac{x(1-x)\rho_0}{n^{\frac{2}{3}}} . \qquad (3.4)$$

Equation (3.4) shows that ρ_C is proportional to $x(1-x)/n^{\frac{2}{3}}$, which appears to be in agreement with the experimental results except for the sample of $Eu_{1-x}Gd_xO$ with $x = 0.25\%$ in Ref. [2].

The large discrepancy of the lightly Gd-doped EuO sample with $x = 0.25\%$ and $n = 0.02\%$ (or carrier density 6×10^{-18} cm^{-3}) [2] from the relationships $\rho_m(0) \propto n^{-\frac{2}{3}}$ and $\rho_C \propto x(1-x)n^{-\frac{2}{3}}$ may be explained in terms of magnetic impurity states and/or the impurity band tail [6]. In the sample of $Eu_{1-x}Gd_xO$ with $x \lesssim 0.5\%$, electrons are semilocalized so that the application of Eq. (2.6) is not appropriate.

Next, we discuss the similarities and differences between Gd-doped and La-doped EuO. Since we do not have any information such as the activation energy for La-doped EuO, we take the same values for Gd-doped and La-doped EuO, that is, $E_C = 0.50\Delta$ for the nondegenerate case and $E_C = 0.15\Delta$ for the degenerate case. In Fig. 6, we show the present result for the lower-energy part of the DOS of $Eu_{1-x}La_xO$ ($E_C = 0.50\Delta$) at paramagnetic temperatures; that of $Eu_{1-x}Gd_xO$ ($E_C = 0.50\Delta$) was presented in the previous study [6]. The energies of the impurity level in Gd-doped and La-doped EuO are estimated to be $\omega_P = -1.0314\Delta$ and $\omega_V = -1.0256\Delta$, respectively. Note that the energy of the bottom of the band with $x = 0.0\%$ in the paramagnetic state is $\omega_b = -1.0231\Delta$. Thus the energy differences between the donor level and the bottom of the conduction band are estimated to be $0.0083\Delta = 0.029$ eV for Gd-doped EuO and $0.0025\Delta = 0.00875$ eV for La-doped EuO. This indicates that the donor level in La-doped EuO is very shallow. There is an impurity band in $Eu_{1-x}Gd_xO$ with $0 \lesssim x \lesssim 0.10\%$, whereas no impurity band substantially appears in $Eu_{1-x}La_xO$. This suggests that in Gd-doped EuO, there is a threshold Gd concentration $x_c(\lesssim 0.1\%)$ for raising T_C, while in La-doped EuO, T_C smoothly increases with increasing La concentration.

Melville *et al.* grew EuO thin films doped with 5% La, Gd and Lu under identical conditions and investigated their magnetic and electronic properties. They found that all three dopants behave similarly despite differences in their electronic configuration and ionic size [3]. For comparison with the experimental observations, in Fig. 7 we show the present results for $M(T)$ and $\rho(T)$ with $x = 5.0\%$ and $n = 1.5\%$. The agreement of $M(T)$ is satisfactory; the values of T_C shown in Fig. 7(a) are 114 K (La) and 122 K (Gd), and the

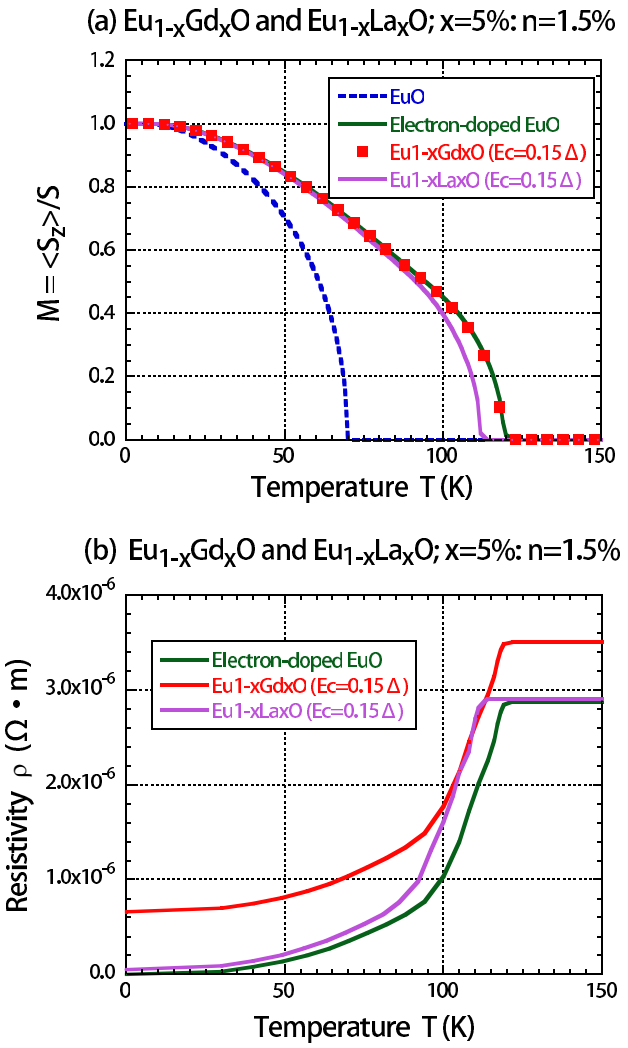

FIG. 7. Results for electron-doped EuO, $Eu_{1-x}Gd_xO$ ($E_C = 0.15\Delta$) and $Eu_{1-x}La_xO$ ($E_C = 0.15\Delta$) calculated with $x = 5.0\%$ and $n = 1.5\%$: (a) $M(T)$ and (b) $\rho(T)$.

experimentally reported values are 116 K (La) and 122 K (Gd). Note that the reduced Heisenberg-type Hamiltonian should be considered instead of H_f for $Eu_{1-x}La_xO$ because La is a nonmagnetic impurity. The difference in $\rho(T)$ between $Eu_{1-x}Gd_xO$ and $Eu_{1-x}La_xO$ shown in Fig. 7(b) is explained by the difference in the nonmagnetic scattering contribution due to the different offset energy. Note that in the ferromagnetic state, an electron with up-spin is subjected to $-IS(=-0.1\Delta)$ at the Eu site, $-IS - E_C(=-0.25\Delta)$ at the Gd site and $-E_C(=-0.15\Delta)$ at the La site. In contrast to the present result, however, the experimental result shows that the nonmagnetic scattering contribution of La-doped EuO is comparable to that of Gd-doped EuO. Furthermore, the value of n for La-doped EuO is reported to be less than half of that for Gd-doped EuO in spite of the same values of x. In cation-doped EuO films, an unknown and uncontrolled concentration of oxygen vacancies is often included, which may be responsible for the disparate results for the nonmagnetic scattering contribution.

IV. SUMMARY

To summarize, in the present study, we have investigated how an attractive potential E_C at the Gd site and low dopant activation affect $M(T)$ and $\rho(T)$ for Gd-doped EuO. Furthermore, by taking an appropriate value for E_C, we have attempted to consistently explain the magnetic and transport properties of rare-earth-doped EuO. The present study has revealed that in degenerate Gd-doped EuO, the effect of E_C on the magnetic curve $M(T)$ is negligible. In contract, the value of E_C has some effect on transport properties while Matthiessen's rule holds. In other words, $M(T)$ is well described by the electron-doped EuO model; $M(T)$ depends on n irrespective of the value of x. The low dopant activation (or $n < x$) is necessary to explain the appearance of the double-dome shape of $M(T)$. The present result supports the picture obtained from the electron-doped EuO model that there is an intrinsic limit to the electron-induced increase in T_C [6]. Owing to the reduction in E_C due to the screening effect, the resistivity is well described by Matthiessen's rule as $\rho(T) = \rho_C + \rho_m(M)$. The amplitude of the change in the magnetic scattering contribution $\rho_m(0)$ is proportional to $n^{-\frac{2}{3}}$ and the nonmagnetic contribution due to the doped rare-earth cation ρ_C is proportional to $x(1-x)/n^{\frac{2}{3}}$, which both appear to be in agreement with the experimental observation of degenerate samples [2,3]. An assumption of low dopant activation of $n = 0.30x$ when $x \lesssim 7.0\%$, while fixing $n = 2.1\%$ for $x \gtrsim 7.0\%$ well explains the dependence of the $\rho(T)$ curve on x that has been experimentally observed for Gd-doped EuO [2]. However, note that the origin of low dopant activation remains an important question. The result for the DOS of $Eu_{1-x}La_xO$ suggests that in La-doped EuO the donor level is so shallow that no impurity band forms and that T_C smoothly increases with increasing La concentration, which is in contrast to Gd-doped EuO. The present result for $M(T)$ well explains the similarities and differences in the experimental observation between Gd-doped EuO and La-doped EuO. On the other hand, the present result for the $\rho(T)$ curve of La-doped EuO is not consistent with the experimental observation. The cause is not clear at this stage; some complex including vacancies may be responsible for the discrepancy [38,39]. Although a high T_C of 200 K has been reported for La-doped EuO [40], the present study suggests that another effect that has not been taken into account in the present models may exist in the sample.

ACKNOWLEDGMENTS

The author sincerely thanks Mr. Yoshio Takahashi for his continuous encouragement.

[1] R. Sutarto, S. G. Altendorf, B. Coloru, M. Moretti Sala, T. Haupricht, C. F. Chang, Z. Hu, C. Schussler-Langeheine, N. Hollmann, H. Kierspel, J. A. Mydosh, H. H. Hsieh, H.-J. Lin, C. T. Chen, and L. H. Tjeng, Phys. Rev. B **80**, 085308 (2009).

[2] T. Mairoser, A. Schmehl, A. Melville, T. Heeg, L. Canella, P. Böni, W. Zander, J. Schubert, D. E. Shai, E. J. Monkman, K. M. Shen, D. G. Schlom, and J. Mannhart, Phys. Rev. Lett. **105**, 257206 (2010).

[3] A. Melville, T. Mairoser, A. Schmehl, D. E. Shai, E. J. Monkman, J. W. Harter, T. Heeg, B. Holländer, J. Schubert, K. M. Shen, J. Mannhart, and D. G. Schlom, Appl. Phys. Lett. **100**, 222101 (2012).

[4] T. Mairoser, F. Loder, A. Melville, D. G. Schlom, and A. Schmehl, Phys. Rev. B **87**, 014416 (2013).

[5] P. M. S. Monteiro, P. J. Baker, N. D. M. Hine, Nina-J. Steinke, A. Ionescu, J. F. K. Cooper, C. H. W. Barnes, C. J. Kinane, Z. Salman, A. R. Wildes, T. Prokscha, and S. Langridge, Phys. Rev. B **92**, 045202 (2015).

[6] M. Takahashi, Phys. Rev. B **86**, 165208 (2012).

[7] M. Takahashi and K. Mitsui, Phys. Rev. B **54**, 11298 (1996).

[8] W. Nolting, G. G. Reddy, A. Ramakanth, and D. Meyer, Phys. Rev. B **64**, 155109 (2001).

[9] C. Santos and W. Nolting, Phys. Rev. B **65**, 144419 (2002).

[10] S. Burg, V. Stukalov, and E. Kogan, Phys. Status Solidi B **249**, 847 (2012).

[11] R. Rausch and W. Nolting, Phys. Rev. B **84**, 184428 (2011).

[12] T. Stollenwerk and J. Kroha, Phys. Rev. B **92**, 205119 (2015).

[13] M. Takahashi, Phys. Rev. B **60**, 15858 (1999).

[14] A. Chattopadhyay, S. Das Sarma, and A. J. Millis, Phys. Rev. Lett. **87**, 227202 (2001).

[15] M. J. Calderón, G. Gómez-Santos, and L. Brey, Phys. Rev. B **66**, 075218 (2002).

[16] M. Takahashi and K. Kubo, Phys. Rev. B **66**, 153202 (2002).

[17] M. Takahashi and K. Kubo, J. Phys. Soc. Jpn. **72**, 2866 (2003).

[18] M. Takahashi, Phys. Rev. B **70**, 035207 (2004).

[19] W. Nolting, T. Hickel, A. Ramakanth, G. G. Reddy, and M. Lipowczan, Phys. Rev. B **70**, 075207 (2004).

[20] F. Popescu, Y. Yildirim, G. Alvarez, A. Moreo, and E. Dagotto, Phys. Rev. B **73**, 075206 (2006).

[21] F. Popescu, C. Şen, E. Dagotto, and A. Moreo, Phys. Rev. B **76**, 085206 (2007).

[22] M. Takahashi, N. Furukawa, and K. Kubo, J. Magn. Magn. Mater. **272**, 2021 (2004).

[23] A.-T. Hoang, Physica B **403**, 1803 (2008).

[24] M. Takahashi, Mater. **3**, 3740 (2010).

[25] P. Wachter, in *Handbook on Physics and Chemistry of Rare Earths*, edited by K. A. Gschneidner and L. Eyring (North-Holland Publishing Company, Amsterdam, 1979), p. 507.

[26] E. H. Hwang and S. Das Sarma, Phys. Rev. B **72**, 035210 (2005).

[27] M. P. Lopez-Sancho and L. Brey, Phys. Rev. B **68**, 113201 (2003).

[28] L. F. Arsenault, B. Movaghar, P. Desjardins, and A. Yelon, Phys. Rev. B **77**, 115211 (2008).

[29] B. Velicky, Phys. Rev. **184**, 614 (1969).

[30] W. Borgiel, T. Herrmann, W. Nolting, and R. Kosimow, Acta Phys. Pol. B **32**, 383 (2001).

[31] See Supplemental Material at http://link.aps.org/supplemental/10.1103/PhysRevB.93.235201 for the derivation of the equation for electronic conductivity, Eq. (2.6).

[32] M. Lipowczan, W. Borgiel, and D. Stysiak, Phys. Status Solidi C **3**, 36 (2006).

[33] C. Haas, Phys. Rev. **168**, 531 (1968).

[34] S. von Molnar and M. W. Shafer, J. Appl. Phys. **41**, 1093 (1970).

[35] M. Takahashi, J. Phys. Soc. Jpn. **80**, 075001 (2011).

[36] A. Mauger, Phys. Status Solidi B **84**, 761 (1977).

[37] M. Takahashi and K. Mitsui, J. Magn. Magn. Mater. **182**, 329 (1998).

[38] D. E. Shai, A. J. Melville, J. W. Harter, E. J. Monkman, D. W. Shen, A. Schmehl, D. G. Schlom, and K. M. Shen, Phys. Rev. Lett. **108**, 267003 (2012).

[39] J. M. An and K. D. Belashchenko, Phys. Rev. B **88**, 054421 (2013).

[40] H. Miyazaki, H. J. Im, K. Terashima, S. Yagi, M. Kato, K. Soda, T. Ito, and S. Kimura, Appl. Phys. Lett. **96**, 232503 (2010).